



Acid-Resistant corrosion protection Polyoxometalate Ionic Liquids as anticorrosion coatings

Abeer Al- Dawsari¹, Aisha M. Turkustani^{1,2} and Fatma Bannani^{1,2*}

¹ Chemistry Department, Faculty of Science for Girls, King Abdulaziz University, P.O. Box 80200, Jeddah 21589, Saudi Arabia

² Chemistry Department, Faculty of Science for Girls, Jeddah University, P.O. Box 80200, Jeddah 21589, Saudi Arabia

Received 05 July 2019,
Revised 11 Oct 2019,
Accepted 13 Oct 2019

Keywords

- Corrosion,
- ionic liquid,
- coating,
- stainless steel,
- polyoxometalate,
- immersion time,
- effect of temperature.

amalturkuestani@kau.edu.sa

Abstract

Metal corrosion is a global problem of worldwide significance affecting many industries. In this research we focus on the use of polyoxometalate ionic liquid hybrid material as corrosion-protection coating of *stainless steel* (SS) alloy surfaces. For this purpose (n-C₇H₁₅)₄N)₅[PW₁₁O₃₉Cu(H₂O)] has been synthesized and characterized by EDS (Energy Dispersive X-ray), FT-IR, UV/Vis, (¹³C, ¹H) NMR spectroscopies and Thermal Gravimetric Analysis. The effect of hydrophobic mixed metal keggin polyoxometalate ionic liquid (POM-IL) as anticorrosion coating of SS surface was investigated in H₂SO₄ solutions by *EIS* and *PDP* electrochemical measurements. The obtained results reveal that POM-IL coating exhibit surface active properties and has fairly good inhibition properties against corrosion of SS in different concentrations of H₂SO₄ solutions, with a protection efficiency $\geq 99\%$. The corrosion rate at different immersion times and temperatures were studied. The results show that, the POM-IL protective coating film remains mostly constant in studied times of immersion and temperatures as witnessed by constant corrosion rates.

1. Introduction

Corrosion is a chemical phenomenon causing disintegration and destruction of the surface and properties of the metal component and structure. It can be also defined as the effect of unwanted chemical reactions on the metals/alloys surface with specific environment [1].

The wide industrial use of *stainless steel* is increasing owing to its interesting properties [2,3]. The main issue with this alloy is, its partial dissolution and surface attack when exposed to aggressive acidic solutions [4]. These acids, such as, sulfuric acid are generally used as acid pickling for corroded metal removal and surface cleaning. The use of coatings as corrosion protection is considered as the most popular method of protecting *stainless steel* and other metals [5]. Many coatings based on organic polymers and inorganic compounds have been reported in the literature [6,7]. However, inorganic coatings are liable to crack and require a high curing temperature [8,9]. Owing to their interesting properties, such as, high stability and low vapor pressure Ionic liquids (ILs) and especially room temperature-ionic liquids (RT-ILs) have been proposed for corrosion-protection coatings [10]. These liquid salts are formed by weak interaction between organic bulk cations and inorganic anions. The use of anionic polyoxometalates (POMs) molecular cluster gave rise to a new family of interesting, polyoxometalate-ionic liquids (POM-ILs) [11].

Polyoxometalates, are molecular cluster formed by early transition metals (Nb, V, W, Mo...) in their highest oxidation states (d⁰, d¹) linked together via oxo (O²⁻) ligands. POMs have relatively low toxicity; their structures remain stable even when accepting electrons (electron reservoir) and form hydrophobic salts with major organic cations. These properties produce them attractive as corrosion inhibitors [12].

Particularly, POM-ILs meet make characteristics of an efficient coating which are hydrophobicity, stability, effective cost, ease of synthesis, non-toxicity, renewability, etc. The use of POM as corrosion inhibitors for Al, Zn, steel and other metals were investigated by many studies [12-19]. Moreover, several patents report formulations containing POMs and/or ILs as anticorrosive agents [20-32]. Recently, POM-ILs were used as coating for copper discs to evaluate the acid-resistance against corrosion by CH₃COOH acid vapors and simulated

“acid rain” [33]. However there was any electrochemical study evaluating the corrosion behavior. In this paper, the synthesis, characterization and application of Room-Temperature hydrophobic polyoxometalates ionic liquid (RT-POM-IL) was reported using electrochemical methods to evaluate the anti-corrosion activity for *stainless steel* in H_2SO_4 solution.

Experimental

All the starting material were obtained from Sigma Aldrich and used as received.

Acidic solutions were synthesized by room temperature dilution of H_2SO_4 analytical grade (1.0 M, 0.75 M, 0.5 M and 0.25 M).

Preparation of Keggin Polyoxometalates Ionic Liquid ($n-C_7H_{15}N$)₅[$PW_{11}O_{39}Cu(H_2O)$]

5.0 g of $Na_2WO_4 \cdot 2H_2O$ was dissolved in 40 mL water under continuous stirring, then, 1.0 g of $CuCl_2 \cdot H_2O$ was added to the solution, a blue precipitate was formed. After addition of 40 mL of 1.0 M H_3PO_4 , the reaction mixture was stirred for additional 10 minutes to dissolve the temporary formed blue solid. Afterwards 2.94 g of tetraheptylammonium bromide ($C_7H_{15}N$)₄Br in 60 mL of toluene was added to the solution. In the separation funnel, the reaction mixture was started to separate into two layers after addition of 60 mL of Toluene. The organic layer was separated, and the solvent was separated under vacuum.

POM-ILs sample was characterized by FTIR spectroscopy using Bruker Tensor II spectrometer. The sample was spreaded between KCl pellets for IR analysis. The obtained spectrum was recorded from 4000 to 400 cm^{-1} with resolution of spectra is 4 cm^{-1} using OPUS Bruker software.

The UV-VIS spectrum was measured over the wavelength ranges from 200 to 800 nm using a Shimadzu UV-1800 spectrometer (Japan), with special spectroscopy software UV Probe version 2.34. Sample was recorded in isopropanol as solvent with cuvettes of quartz (optical path length equal 1.0 cm).

¹H/¹³C-NMR: the spectra were recorded with Bruker AV-400 MHz multi nuclear probe spectrometer. Chemical shifts (δ in ppm) are listed and refer to the not deuterated part of the used solvent [(C_3D_6O)] at 2.05ppm, and ¹³C NMR spectra were referenced similarly to the peak in the centr of the CD_3 septet of $(CD_3)CO_2$ at 29.8 ppm and singlet of CO at 206.35.

TGA analysis of keggin POM-IL hybrid was performed on a Thermo-Microbalance TG 209 F3 (NETZSCH) instrument. The sample was kept under a mixture of N_2 (20 ml/min) and He (10 ml/min) at 10° C/ min heating rate. The EDS data were obtained and treated by using the TIA software (Tecnai Imaging and Analysis software version 1.9.162) and Gatan Micrograph Software version 2.3.

SEM analysis was performed by means of scanning electron microscopy field emission (FEG-SEM, Quanta FEG450, FEI, the Netherlands) using an ETD Everhart Thornley detector (High Vacuum mode), a solid-state backscattering electron detector (VCD) and EDS detector (XFLASH6-30, Bruker) for elemental analysis.

Specimen Preparation and Surface Pretreatment

The SS (302L) specimen was cut in the form of a small rectangular sheets (1.5 cm x 3.0 cm x 3.0 mm). The composition of the SS electrode is Mn: 0.900%, Cr: 18.81%, Ni: 7.336% and Fe: 72.94%. Before exposure, the specimen was polished with four grades of emery papers 600, 800, 1000 and 1200, subsequently washed with bi-distilled water and acetone. All experiments were done in freshly prepared solutions.

SS specimen Coating: The stainless steel rectangular sheets were sonicated in $(CH_3)_2CO$ for 10 min and thoroughly wash with acetone. After air-drying the specimen surfaces were coated by dipping the SS sheets in freshly prepared room temperature POM-IL.

Electrochemical measurements

The electrochemical behavior for SS sample in the presence and absence of POM-ILs was conducted using a conventional three-electrodes immersed in solution with glass cell assembly at room temperature using an ACM potentiostat with EIS software. Stainless steel specimen of dimension (3.0 x 1.5 x 0.3 cm^3) as the working electrode, Pt as auxiliary electrode and Ag/AgCl as a reference electrode. All the experiments were carried out at 25 °C in H_2SO_4 solutions by immersing 1.0 h.

Impedance measurements (EIS)

The impedance was done at the *open circuit potential (OCP)* using AC signals of 10^{-2} V amplitude over the frequency ranging from 0.5 Hz-100 kHz at OCP. The parameters obtained from the Nyquist plots are R_{ct} (*resistance charge transfer*) which were obtained from the diameter at high frequency loop of the semicircles and the capacity of *double layer*.

$$C_{dl} = \frac{1}{2\pi f_{\max} R_{ct}} \quad (1)$$

where *charge transfer resistance* is R_{ct} and *double layer capacitance* is C_{dl} . The experiment was done in the absence and presence of POM-ILs coating.

The inhibition efficiencies were calculated from the R_{ct} and/or C_{dl} values according to Equations (2&3):

$$IE\% = \frac{R_{ct} - R_{ct}^{\circ}}{R_{ct}} \times 100 \quad (2)$$

$$IE\% = \frac{C_{dl}^{\circ} - C_{dl}}{C_{dl}^{\circ}} \times 100 \quad (3)$$

where R_{ct}° and R_{ct} are the *resistance of charge transfer* in the presence and absence of coating and C_{dl}° and C_{dl} are the *capacitance of double layer*, respectively.

Potentiodynamic Polarization (PDP)

The PDP measurements were done from cathodic to an anodic potential after the impedance experiment, at 1mV/s sweep rate and through the range -800 mV to +100 mV, a steady potential is established. The electrode under examination was polarized and both *cathodic* (β_c) and *anodic* (β_a) curves were registered, respectively. The linear anodic and cathodic lines were extrapolated to the potential to obtain I_{corr} . The IE% was obtained from I_{corr} values by the equation:

$$IE\% = \frac{I_{corr}^{\circ} - I_{corr}}{I_{corr}^{\circ}} \times 100 \quad (4)$$

where I_{corr} and I_{corr}° are the *current densities* in the presence and absence of coating, respectively.

The SS sample was left in test solution for 1.0 h approximately, before performing the electrochemical measurements, at *open-circuit potential (OCP)* until a steady state was established. All the experiments, have been reported twice under the same conditions in order to assure measurements reproducibility and reliability.

Results and Discussion

The anionic cluster was balanced the charge with tetraheptylammonium cations and transferred to organic phase by anion metathesis. The phase transfer was achieved by put the polyoxometalate solution on the tetraheptylammonium-bromide which dissolved in toluene.

The pairing of Keggin polyanion with the bulky organic tetraheptylammonium cation has led to the formation of hydrophobic organic-inorganic hybrid (RT-POM-IL). The formula obtained from the EDS elemental and TGA analysis of the sample gives empirical structure of $(n\text{-}C_7H_{15})_4N)_5[PW_{11}O_{39}Cu(H_2O)]$

IR spectroscopy

The IR spectroscopy is useful for structural identification and changes in the Keggin polyoxometallic framework. The spectrum of $\{PW_{11}CuO_{40}\}$ (Fig. S1) presents the characteristic bands of the Keggin framework observed at 958, 871, 792, which can be respectively ascribed to stretching modes of the terminal $W-O_t$ ($\nu_{\text{sym}} W=O_t$), $W-O_c-W$ inter bridges between corner-sharing WO_6 octahedra ($\nu_{\text{sym}} W-O_c-W$), intra bridges between edge-sharing WO_6 octahedra $W-O_b-W$ ($\nu_{\text{sym}} W-O_b-W$). The asymmetric vibrations of P-O ($\nu_{\text{asym}} P-O$) of the tetrahedral PO_4 were found at 1095 and 1024 cm^{-1} .

The latter feature is splitted by comparison with the P–O stretching ($\sim 1083\text{ cm}^{-1}$) of the parent $\text{PW}_{12}\text{O}_{36}$ Keggin structure. Similar results were reported in the case of introduction of vanadium into Keggin polyoxometalate [34]. The introduction of copper into the framework of the polyoxometalate led to splitting of the P–O, as well as, a shift of the main *FTIR* bands which is the consequence of the reduced symmetry.

Moreover, the bands of absorption at 697 cm^{-1} is assigned to the characteristic peak of Cu–O ($\nu_{\text{aaaa}}\text{ Cu-O}$) vibrations in the POM lattice. The tetraheptyl ammonium cations $[(\text{n-C}_7\text{H}_{15})_4\text{N}]^+$ are revealed by their characteristic C–H symmetric and asymmetric stretching vibrations (around $2950\text{--}2860\text{ cm}^{-1}$). Moreover, the CH_3 group is evidenced by the bands at (around $1460\text{--}1480\text{ cm}^{-1}$) and 1380 cm^{-1} , respectively assigned to the C–H deformation vibrations and symmetric deformation. The relatively weak band at 730 cm^{-1} is ascribed to the CH_2 rocking vibration.

IR analysis shows that the basic Keggin structure is maintained in the POM-IL hybrid.

UV-Vis spectroscopy

It is known that when POM, based on transition metal in their highest oxidation states, are irradiated with *UV* light, they exhibit strong absorption features in the *UV* area below 400 nm.

These absorptions can be assigned to oxygen-to-metal (O \rightarrow M) bands of charge transfer LMCT (Ligand to Metal Charge Transfer). Electrons are transfer from the occupied electronic states of low energy (oxygen 2p orbitals in polyoxoanions) to the vacant states of high-energy (metal d orbitals).

The phosphorus mono copper tungstic Keggin cluster $\{\text{PCuW}_{11}\text{O}_{40}\}$ exhibits absorption top peaks at 238 and 273 nm. These features are attributed to the intramolecular (O_t \rightarrow W and O_{b,c} \rightarrow W) ligand to the charge transfer of metal transitions (LMCT) (Fig. S2). In addition, the spectrum presents a weak absorption peak in the visible spectrum at around 780 nm. This absorption is due to d-d transition of the copper hetero d-element. A comparison with the *UV-vis spectrum* of the well-known copper hexaqua complex shows an interesting similarity about the absorption in the visible spectral range occurring at around 800 nm and explains the turquoise color of the hybrid compound. This comparison indicates that the copper retains its octahedral coordination environment in the organic phase with a sixth coordination position bounded to a water ligand (5 oxygen by the Keggin cluster and the sixth oxygen bonding aqua ligand). Similar results were obtained with $\{\text{SiW}_{11}\text{O}_{39}\text{Cu}(\text{H}_2\text{O})\}$ [33].

NMR spectroscopy

The n-Hep₄N⁺ cation showed the ¹H *NMR* resonances at 0.62 (12H, H7), 1.07–1.8 (40 H, H2–H6), and 3.14 (8H, H1) ppm in C₃D₆O versus tetra methyl silane (TMS). ¹³C{¹H} *NMR* observed resonances for the n-Hep₄N⁺ cation were typically at 59 (C1), 32.1 (C5), 29.3 (C4), 26.6 (C2), 23 (C3), 22.3 (C6) and 14.3 (C7) ppm. (Fig S3, S4)

Thermogravimetric analysis

The thermal stability of the Keggin POM-IL hybrid was studied by *TGA* analysis. The *TGA* curve is shown in figure 1. In a first step (T < 210 °C), residual solvent and cluster-based water-ligands are lost (mass loss ca. 4.9%). The mass loss (42,6 %) observed between ca. 210 to 440 °C is essentially due to the decomposition of the organic cation.

SEM and EDS characterization

Surface characterization studies were conducted in order to estimate and compare the extent damage by corrosion in the presence and absence of POM-ILs, which gave concept about the extent of protection occur by the hydrophobic POM-ILs coating. This analysis was performed using *SEM/EDS* techniques.

SEM was performed on the POM-ILs coated *stainless steel* surface. The images obtained for uncoated and POM-ILs coated *SS* material are shown in Fig. 2.

The *SEM* topography of the POM-ILs forms a smooth, compact and uniform surface film on the surface of *stainless steel* sheet. After 1.0 h of immersion in a 1.0 M solution of sulfuric acid during 1.0 h, it can be easily seen from the *SEM* image of coated metal sheets Fig. (2-d) that the metal surface is still smooth which confirms that the coating is still present on the *SS* sample surface.

EDS analysis confirms the keggin structure of the POM-ILs in which W/Cu and W/P molar ratios are 11/1. (Fig. S6)

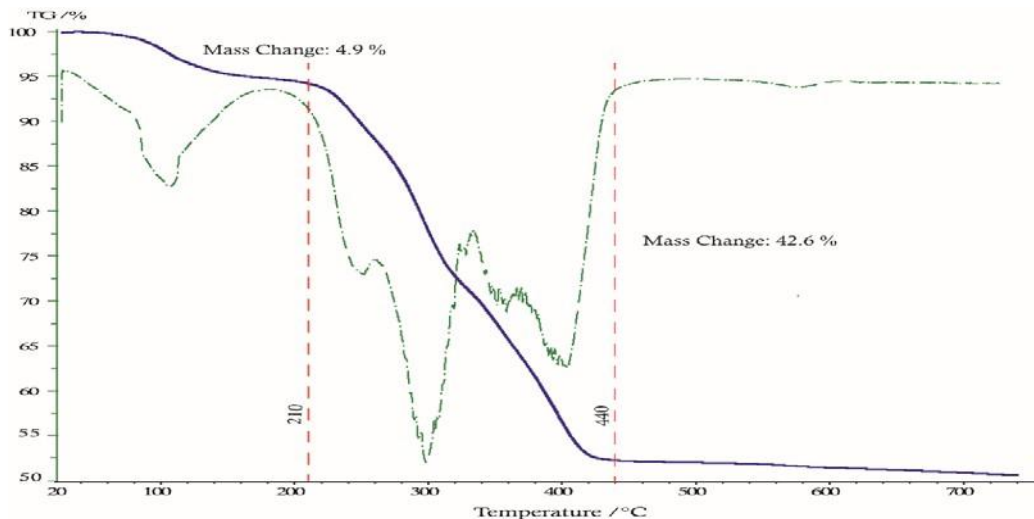


Figure 1: Thermal gravimetric analysis of $(n\text{-C}_7\text{H}_{15})_4\text{N})_5[\text{PCuW}_{11}\text{O}_{40}]$. Relative mass m/m_0 as function of temperature (blue line) and its first derivative (green line)

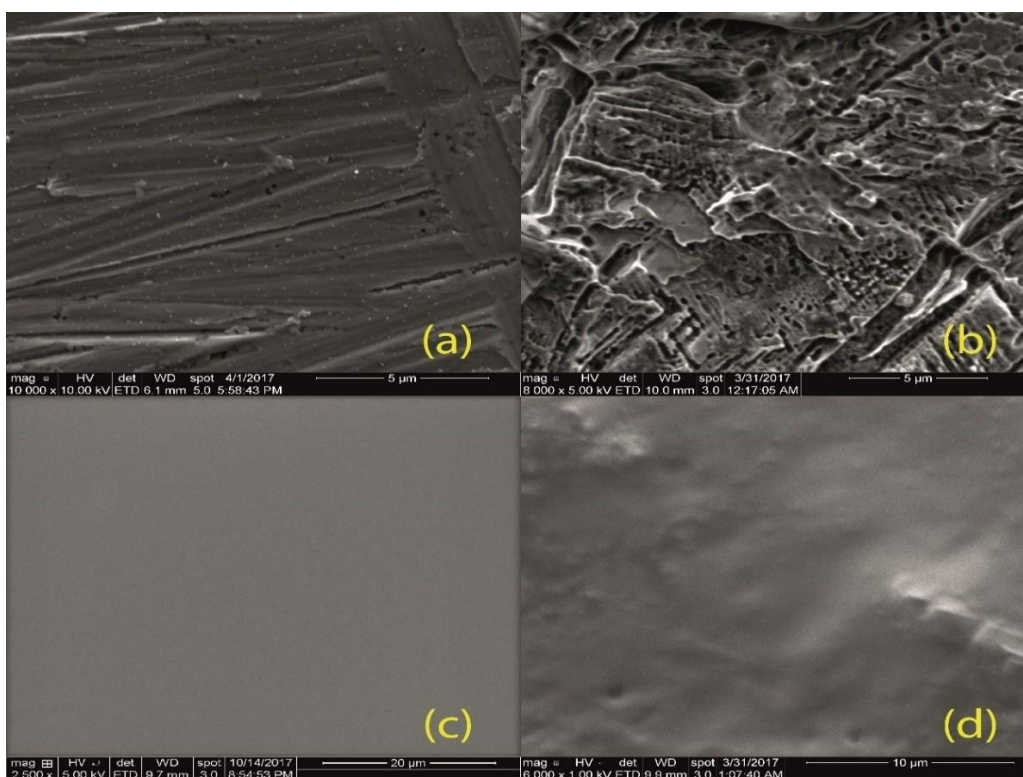


Figure 2: SEM images of (a) blank SS, (b) blank SS after immersion for 1.0 h in 1.0 M H_2SO_4 . (c) $((\text{C}_7\text{H}_{15})_4\text{N})_5[\text{PW}_{11}\text{O}_{39}\text{Cu}(\text{H}_2\text{O})]$ hybrid molecular Material coating on SS metallic surface before immersion in H_2SO_4 . (d) coated after immersion for 1.0 h in 1.0M H_2SO_4

Application of POM-ILs as acid-resistant coating

The active effect of POM-ILs on the SS behavior in sulphuric acid (H_2SO_4) solutions have been studied using *electrochemical* measurements which are:

1- Effect of H_2SO_4 concentrations at 25°C

1-1 Electrochemical Impedance Spectroscopy (EIS) Measurements

EIS is a powerful tool to evaluate the protective properties of coating film on metal surface [35]. It has the advantage to provide information on the surface of metal sample and rapid determination of corrosion rate. EIS was performed at room temperature (25° C) for SS in various concentrations of H_2SO_4 acid solutions in the presence and absence of POM-ILs coating.

Figure 3 illustrates Nyquist plots obtained from *EIS* measurements for *SS* sample in the presence and absence of POM-ILs coating in 0.25, 0.5, 0.75 and 1.0 molar sulfuric acid solutions. These figures illustrated that the impedance diagrams have mainly a semi-circle in low concentrations (0.25M, and 0.5M) of H_2SO_4 but in the high concentrations (0.75M and 1.0M) of H_2SO_4 , the curves are not perfect semi-circle especially in the presence of POM-ILs coating. The deviation from perfect semicircle is attributed to non homogenous surface, also to the frequency scuttle and mass transfer resistant and to the aggressive attack to *SS* surface by high concentrations of H_2SO_4 acid solution [36-39]. The semi-circle appearance indicates that the presence of POM-ILs coating inhibit the dissolution of *SS* sample at all concentrations of H_2SO_4 solutions.

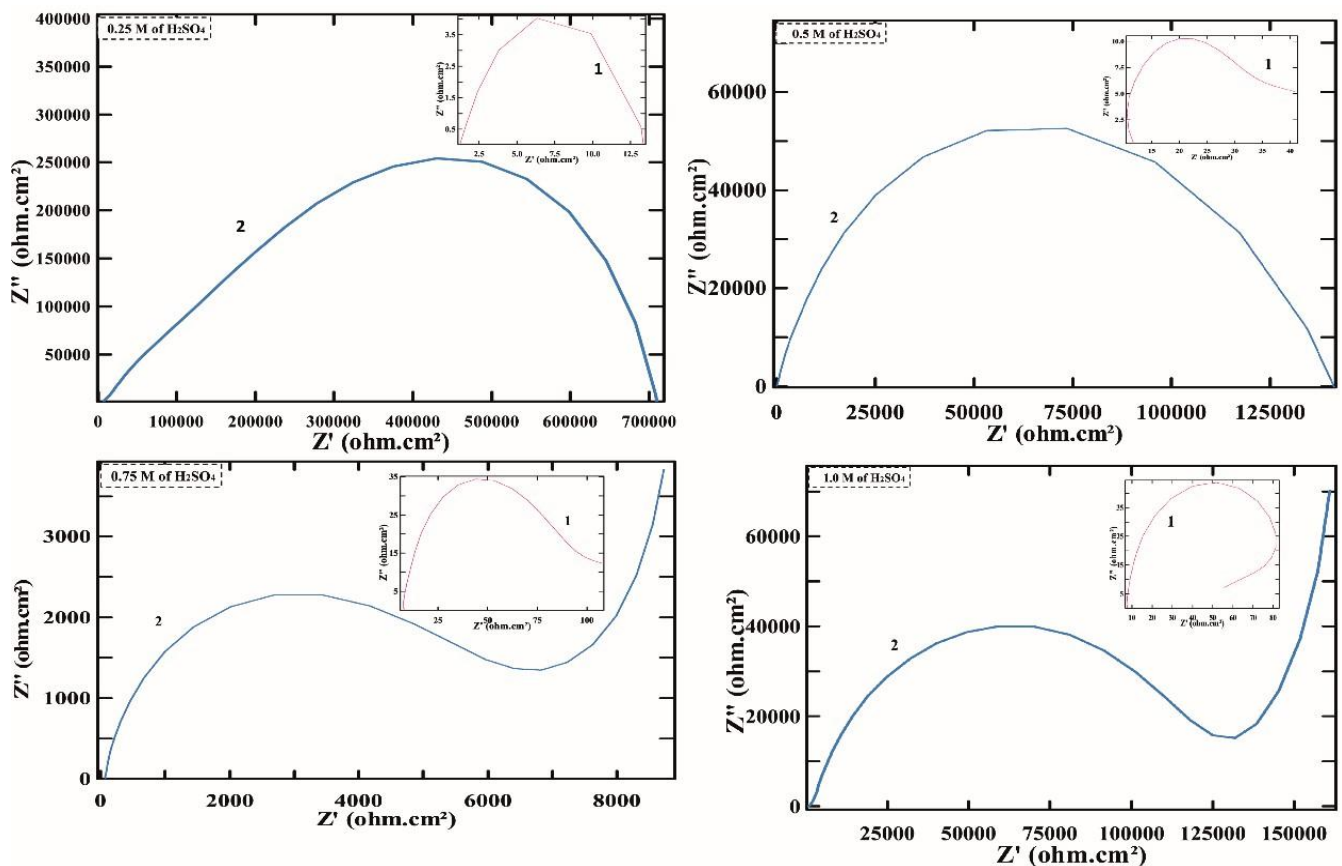


Figure 3: Nyquist plots of *EIS* measurements of *SS* after 1.0 h immersion in various concentrations of H_2SO_4 at 25 °C.
(1): in the absence, (2): the presence of [POM-ILs].

The impedance plot displays two capacitive loops, the loop at high frequency is related to R_{ct} values which traduces the resistance between Helmholtz plane and the metal surface were obtained from the differences between lower and higher frequencies [40] using Stern-Geary Equation (1) and then get the corrosion current. The second loop in the low-frequency domain represents the relaxation of intermediates adsorbed on the *SS* surface. These intermediate compounds contain $[FeOH]_{ads}$ and $[FeH]_{ads}$. The strong acids and in the area near OCP of corrosion, both dissolution (anodic) and H_2 evolution (cathodic) reactions occur at the same time on the *SS* surface[41].

It is obvious from Figure 3 that *SS* corrosion rate in different concentrations of sulfuric acid decreases as increasing the acid concentration, and the dependence R_{ct} and constant phase element C_{dl} (*CPE*) values in H_2SO_4 acid concentration could be to some extent explained by the change in physical properties of the sulfuric acid when alteration in concentrations, this can be attributed to the changes in the mechanism conductivity and viscosity at high and low concentrations of H_2SO_4 [42].

The high viscosity prevent the diffusion of products from anode section on the *SS* surface to the bulk of the solution and block the *SS* surface and hinder the hydrogen bubbles release from the cathode section.

Thereover, Lewis et al. [43] inspected the effect of the chromium content of the *SS* sample (18.81%) on their corrosion behavior in acidic media. The variation in the corrosion rate by changes in H_2SO_4 concentrations may be attributed to the $FeSO_4$ quantity collected on the *SS* surface as corrosion residues at high concentrations.

Also, it is seen that the diameter of semicircle of Nyquist plots increases in the presence of coating with POM-ILs in all concentrations of sulfuric acid solutions which suggests that POM-ILs induced inhibition against corrosion of SS due to the covering layer on the metal surface which protect the SS surface from corrosion.

The parameters R_{ct} , $C_{dl}=CPE$ were obtained and listed in Table (1). CPE is replaced for the capacitive element to give a correct fit, as the take out capacitive loop is not regular semicircle (depressed semicircle). The CPE is a special element whose the phase is separate and independent on frequency and whose the value of impedance is a function of the angular frequency (ω).

It can be seen from this Table that R_{ct} values for coated SS sample with POM-ILs are higher than that of uncoated sample in all studied concentrations of H_2SO_4 solutions, this indicates that the corrosion rate decreased due to less active site available for charge transfer, which implies that the studied POM-ILs inhibits *stainless steel* corrosion. This is confirmed by decreasing in CPE values.

Table 1: Corrosion parameters obtained from *EIS* of SS electrode at various concentrations of H_2SO_4 in the presence and the absence of POM-ILs at 25°C.

Concentration		R_{ct} ($\Omega\text{ cm}^2$)	CPE ($F\text{ cm}^{-2}$)	$IE_{R_{ct}}\%$	$IE_{CPE}\%$
0.25 M	Blank	12.22	9.413×10^{-4}	--	--
	POM	7.745×10^5	1.882×10^{-7}	99.99	99.98
0.5 M	Blank	20.76	4.672×10^{-4}	--	--
	POM	1.51×10^5	3.330×10^{-7}	99.98	99.93
0.75M	Blank	78.90	3.748×10^{-4}	--	--
	POM	6.16×10^3	3.080×10^{-7}	98.71	99.91
1.0 M	Blank	85.68	9.279×10^{-5}	--	--
	POM	1.207×10^3	1.238×10^{-7}	99.92	99.87

Inhibition percentage efficiencies ($IE_{R_{ct}}\%$ and $IE_{CPE}\%$) obtained from *EIS* measurements are calculated from equations (2&3) and recorded in Table 1. It is clear that the $IE_{R_{ct}}\%$ and $IE_{CPE}\%$ values is approximately the same in all concentrations of H_2SO_4 solutions under this study which shows that the POM-ILs coated the SS surface is not affected by the variation of acid concentrations.

1-2 Polarization (PDP) Measurements

The *PDP* curves for SS sample in 1.0 M H_2SO_4 in the presence and absence POM-ILs coating after immersion for 1.0 h at 25 ± 0.1 °C are illustrate in Fig.4. Corrosion kinetic parameters such as E_{corr} , I_{corr} , β_a and β_c were obtained using ACM analysis software and recorded in Table 2.

$IE_{PDP}\%$ was calculated from the experimental I_{corr} value (99.99%) using the equation (4). The displacement of both cathodic and anodic lines shows that POM-ILs delays the cathodic (hydrogen evolution) and the anodic (metal dissolving) processes (Fig. 4), i.e., these POM-ILs acts as mixed inhibitor. This behavior was observed previously in other studies [44-46].

It is clear from Table 2 that there is displacement in the E_{corr} value in the presence of POM-ILs to less negative (more positive) value and a decrease in I_{corr} , i.e., decrease in corrosion rate by shifting the cathodic and anodic line curve to lower I_{corr} . with regard to the free acid solution (1.0 M H_2SO_4) are indicative of decrease in corrosion rate, suggests that POM-ILs blocked the active region on SS surface and has acted as a hinders for oxidizer species, this means that that the studied POM-ILs inhibit the dissolution of SS and slower the cathodic reduction reaction relative to the hydrogen gas evolution. $IE\%$ value close to 99.99%, meaning that the efficient adsorption of the hydrophobic film over the SS surface, and SS without surface treatment has the lowest corrosion resistance and highest corrosion rate in the 1.0 M H_2SO_4 acid solution [40,43].

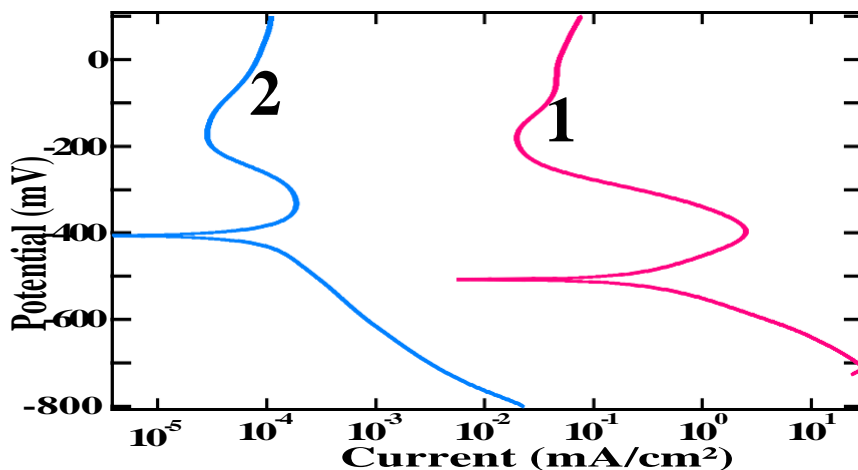


Figure 4: Potentiodynamic polarization plots for SS sample in 1.0 M H₂SO₄ (1): in the absence and (2): the presence of [POM-ILs]

Table 2: Corrosion parameters obtained from PDP for SS electrode at various concentrations of H₂SO₄ in the absence and the presence of POM-ILs at 25°

Concentration		$-E_{corr}$ (mV/SCE)	β_a (mV/decade)	$-\beta_c$ (mV/decade)	I_{corr} (μ A/cm)	$IE_{I_{cor}}$ %
1.0 M	Blank	508.43	151.16	120.35	1.496	--
	POM	405.98	97.92	113.3	1×10^{-4}	99.99

2- Effect of immersion time

The corrosion action of SS sample in 1.0 M H₂SO₄ solution in the absence and presence of POM-ILs coating at different immersion times (1, 2, 24 and 168 h) were investigated by the EIS and PDP measurements at room temperature (25°C).

2-1 EIS Measurements

The representative Nyquist curves of *stainless steel* in 1.0 M H₂SO₄ solution in the presence and absence of POM-ILs coating after (1.0 – 168.0 hours) are given in Fig. 5. Nyquist plots of SS in 1.0 M H₂SO₄ does not yield perfect semicircle as expected from the EIS theory.

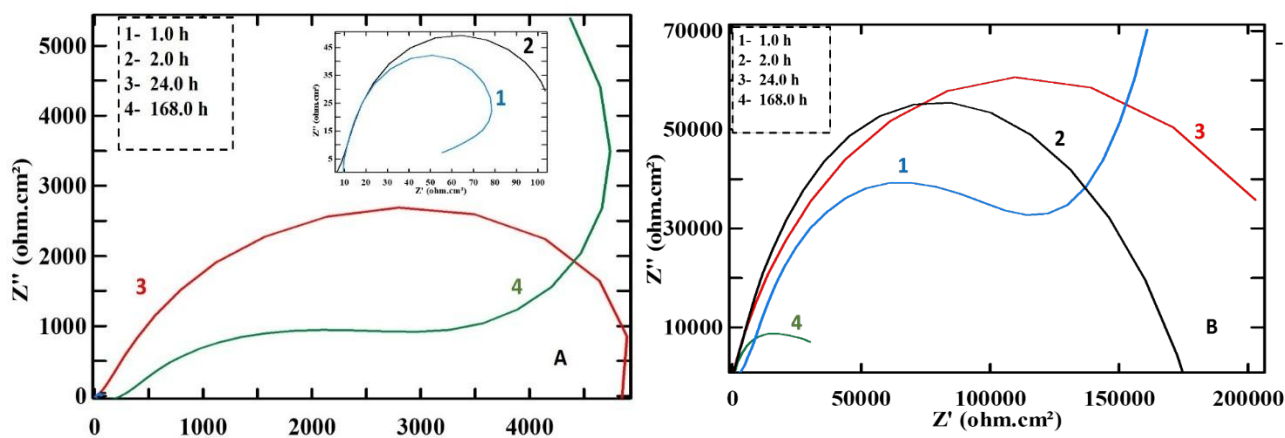


Figure 5: Nyquist curves for SS in different time of immersion in 1.0 M of H₂SO₄ at 25 C°. (A): in the absence, (B): the presence of [POM-ILs]

Table 3: Corrosion parameters obtained for SS electrode at different times of immersion in H₂SO₄ in the absence and the presence of POM-ILs at 25°C.

Concentration		R _{sol}	R _{ct} (Ω cm ²)	C _{dl} (F cm ⁻²)	IE _{Rct} %	IE _{Cdl} %
1.0 h	Blank	9.683	8.684×10 ¹	1.170×10 ⁻⁴	--	--
	POM	1.581×10 ³	1.207×10 ⁵	1.816×10 ⁻⁷	99.93	99.85
2.0 h	Blank	7.013	1.109×10 ²	9.279×10 ⁻⁵	--	--
	POM	3.473×10 ²	1.562×10 ⁵	1.238×10 ⁻⁶	99.93	98.67
24.0 h	Blank	8.526	6.223×10 ³	9.825×10 ⁻⁶	--	--
	POM	3.139×10	2.348×10 ⁵	2.836×10 ⁻⁶	97.33	97.11
168.0 h	Blank	2.327×10 ²	3.789×10 ³	1.570×10 ⁻⁵	--	--
	POM	4.424×10 ²	3.669×10 ³	7.199×10 ⁻⁶	3.271	1.181

A depressed shape in Nyquist plot denotes that the process of SS corrosion in 1.0 M H₂SO₄ is controlled by a charge transfer process [47-52]. The diameter of semi-circle increased after the coating with POM-ILs at all immersion times. The impedance parameters R_{ct} and C_{dl} are calculated and recorded in Table 3. Results show that C_{dl} values with POM-ILs coating are lower than those without coating. This can be attributed to the protective film of POM-ILs on the surface of SS sample which are stable with the variation of immersion time until 24h then the film is dissolved after 186h. Also, R_{ct} values increase in the presence of POM-ILs coating, as witnessed by the increase in the diameter of the semicircles. R_{ct} , as well as, $IE_{Rct}\%$ values approximately remain constant in the immersion times 1.0, 2.0 but it decreases with increasing immersion time at 24.0 and 186h showing that the POM-ILs coating remains stable at low immersion times but it becomes unstable at high immersion time.

2-2 PDP Measurements

The polarization diagrams and the parameters values of SS sample immersed in 1.0 M H₂SO₄ solution are illustrated in Figure 6 and Table 4. It is evident from figure 6 that the presence of POM-ILs shifts the E_{corr} values toward less negative (more positive) direction at studied immersion times. This behavior reflects the inhibitive action of POM-ILs coating. The I_{corr} values vary with increasing immersion time in the presence of POM-ILs coating compared with those without coating. The curves of anodic and cathodic plots are shifted to lower values of I_{corr} , meaning that the hydrogen evolution and the dissolution of SS sample are inhibited due to the protective behavior of POM-IL coating [53]. The slopes of both anodic and cathodic lines (β_a , β_c) were relatively modified on rising the immersion time, this means that both reactions (dissolution of metal and H₂ evolution) are affected, and that POM-ILs coating is considered as a mixed inhibitor in all studied immersion times. $IE_{PDP}\%$ values remain constant with increasing immersion time until 24h then it decreases and gives an acceleration in corrosion after 168h. Similar results were presented in EIS measurements.

1- Effect of temperature

It is well known that temperature is the factor that affect the behavior of metals in a corrosive media and it also can modify the interaction between metal and inhibitor.

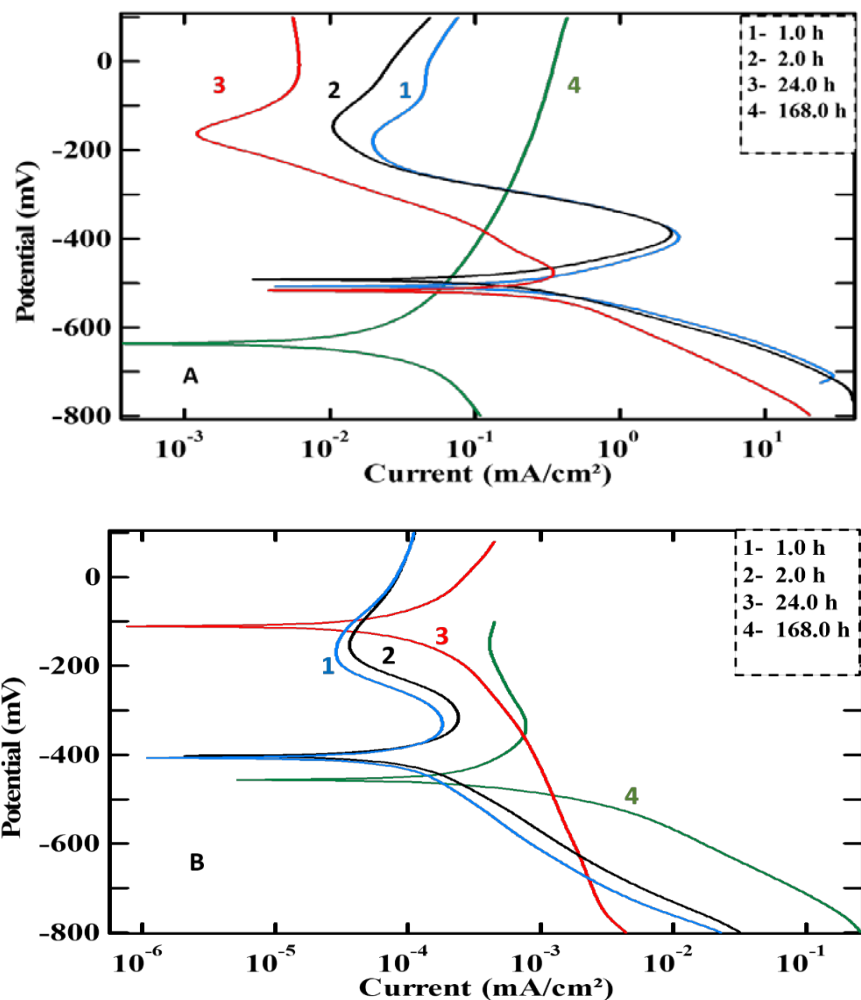


Figure 6: Polarization curves of SS in different times of immersion in 1.0 M of H₂SO₄ at 25°C (A): in the absence, (B): the presence of [POM-ILs]

Table 4: Corrosion parameters obtained from PDP of SS electrode at different times of immersion in H₂SO₄ in the presence and absence of POMs at 25°C

Immersion of time		$-E_{\text{corr}}$ (mV/SCE)	β_a (mV/decade)	β_c (mV/decade)	I_{corr} ($\mu\text{A}/\text{cm}$)	IE_{Icor} %
1.0 h	Blank	508.4	151.1	120.3	1.4960	--
	POM	405.98	97.92	113.3	1.0×10^{-4}	99.99
2.0 h	Blank	482.6	151.4	98.61	0.6950	--
	POM	400.7	93.63	100.8	18×10^{-4}	99.74
24 h	Blank	509.8	110.5	56.11	0.1680	--
	POM	147.9	107.3	100.3	6.092×10^{-5}	99.96
168 h	Blank	640	471	7.78	0.0019	--
	POM	456.53	288.21	61.02	0.0050	-1.68

3-1 Electrochemical Impedance Spectroscopy (EIS) Measurements

Figure 7 and Table 5 summarize the experimental EIS results obtained for SS corrosion in the presence and absence of POM-ILs in 1.0 M H₂SO₄ at the temperature range (25- 60°C). A considerable increase in the total impedance was observed in the presence POM-ILs at all temperatures. C_{dl} values increase with increasing temperature, due to a decreased in the homogeneity of the adsorbed POM-ILs film. From the Table 5, R_{ct} values generally increase with increasing temperature.

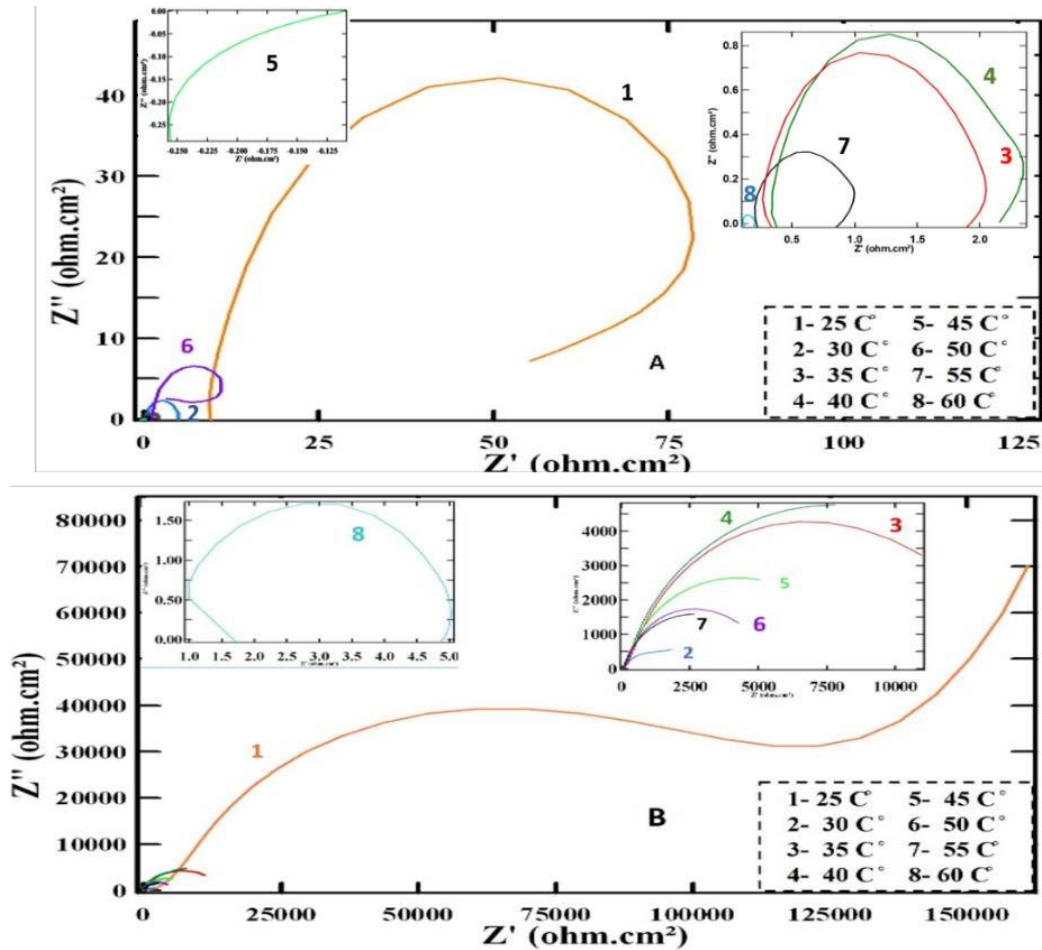


Figure 7: Nyquist plots of SS in 1.0 M H_2SO_4 at several temperatures. (A): in the absence, (B): the presence of [POM-ILs]

Table 5: Parameters obtained from *EIS* of SS electrode at 1.0 M H_2SO_4 in the presence and absence of POM-ILs at various temperatures

Temperature		R_{ct} ($\Omega \cdot cm^2$)	C_{dl} ($F \cdot cm^2$)	IE_{Rct} %	IE_{Cat} %
25°C	Blank	8.684×10^1	1.170×10^{-4}	--	--
	POM	1.207×10^5	1.816×10^{-7}	99.92	99.85
30°C	Blank	4.936	3.665×10^{-3}	--	--
	POM	1.129×10^3	2.057×10^{-5}	99.56	99.44
35°C	Blank	1.953	5.173×10^{-3}	--	--
	POM	1.401×10^4	4.396×10^{-5}	99.99	99.15
40°C	Blank	2.043	5.335×10^{-3}	--	--
	POM	7.418×10^3	4.739×10^{-5}	99.97	99.11
45°C	Blank	3.073×10^{-2}	6.099×10^{-3}	--	--
	POM	4.657×10^3	6.100×10^{-5}	99.99	99.00
50°C	Blank	1.299×10^1	3.817×10^{-3}	--	--
	POM	4.991×10^3	9.744×10^{-5}	99.74	97.45
55°C	Blank	7.945×10^{-1}	6.755×10^{-3}	--	--
	POM	1.993×10^3	1.331×10^{-4}	99.96	98.02
60°C	Blank	9.606×10^{-2}	8.337×10^{-2}	--	--
	POM	1.651	2.371×10^{-3}	94.18	97.16

3-2 PDP Measurements

Figure 8 shows the polarization plots for SS sample in 1M H₂SO₄ solution at different temperatures.

Tafel curves shifted to the right side with increasing temperature (Figure 8-B). This behavior can be attributed to the effect of current density on corrosion when the temperature was increased from 25 to 60 °C and may be also ascribed to coating dissolution as increasing temperature. From Table 6, E_{corr} , β_a and β_c vary with rising temperature. The inhibition efficiency remains approximately stable up to a temperature of 40° C and after that there was a decline from 45°C to 60°C. Maximum inhibition efficiency was found to be 99.98% at 25 °C and minimum of 82.24% at 60 °C.

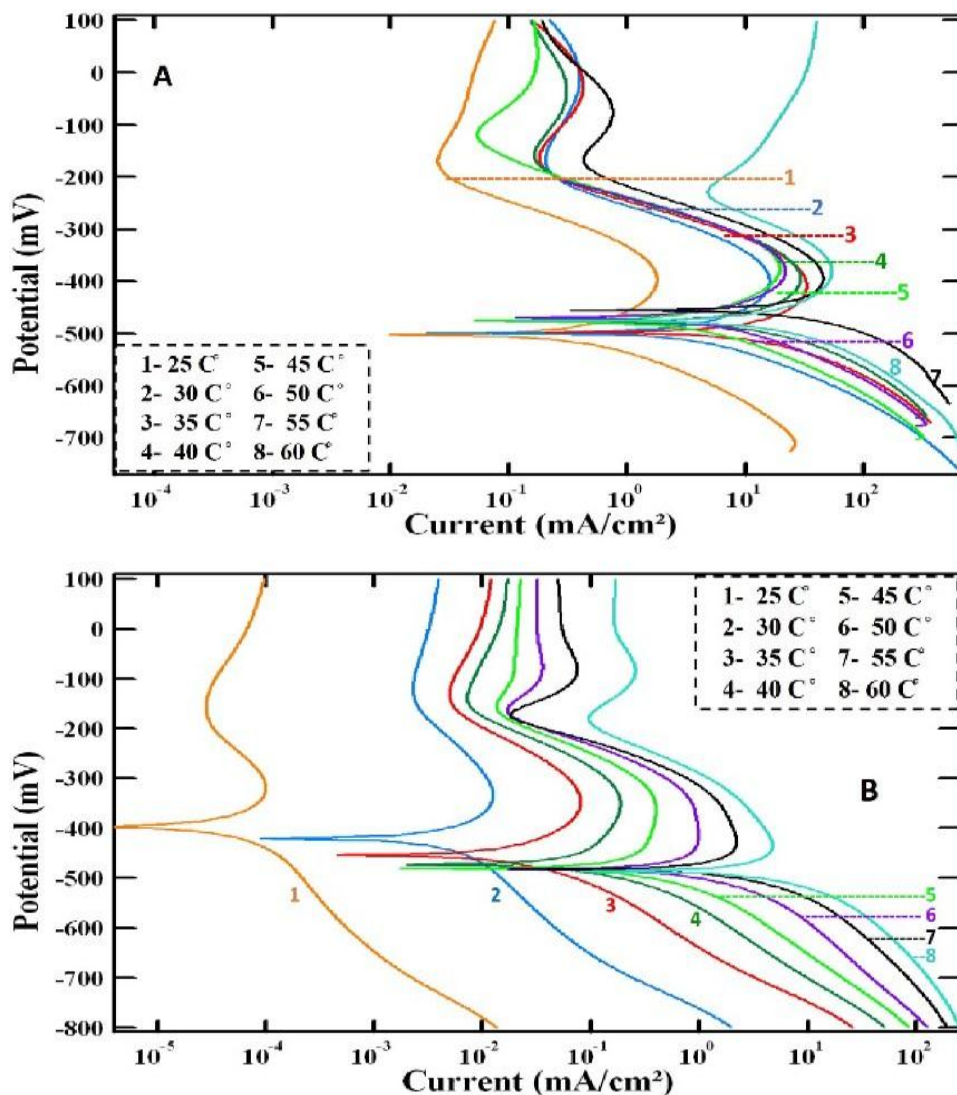


Figure 8: PDP curves for SS electrode in 1.0 M H₂SO₄ at several temperatures. (A): in the absence, (B): the presence of [POM-ILs]

The effect of temperature can be explained by the fractional desorption of the coating from the surface of metal. The same results were obtained by Ergun et al. 2008 [54], who attributed the decrease in IE% with rising temperature to the dissolution of SS in acidic environment and/or the desorption of the inhibitor from metal surface.

Application of Arrhenius equation

The apparent activation energy (E_a) associated with SS corrosion in acidic solution in the presence and absence of POM-IL was determined using Arrhenius plot. To calculate the activation parameters of the corrosion process and to study the inhibition mechanism due to the temperature, polarization measurements were performed at 298 K, 303 K, 308 K, 313 K, 318 K, 323 K, 328 K and 333 K range of temperatures, in the absence and presence of POM-ILs.

Table 6: Corrosion parameters obtained from PDP of SS electrode at 1.0 M H₂SO₄ in the presence and absence of POM-ILs at different temperatures

Temperature		$-E_{corr}$ (mV/SCE)	β_a (mV/decade)	$-\beta_c$ (mV/decade)	I_{corr} (μ A/cm)	$IE_{I_{corr}}$ %
25° C	Blank	508.4	151.1	120.3	14.96	--
	POM	405.98	97.92	113.3	0.003	99.98
30° C	Blank	499.3	137	95.34	15.31	--
	POM	420.4	89.84	89.17	0.004	99.97
35° C	Blank	503.4	218.4	114.5	19.04	--
	POM	459.3	81.93	62.63	0.055	99.71
40° C	Blank	483.4	207.3	115.02	19.09	--
	POM	469.9	92.72	54.37	0.105	99.45
45° C	Blank	477	164.4	115.7	19.30	--
	POM	492.9	250.6	59.85	0.930	95.18
50° C	Blank	466.7	182	133.7	25.00	--
	POM	487.7	116.8	62.88	1.111	95.56
55° C	Blank	470.2	242.3	71.71	27.02	--
	POM	495.4	136	70.33	2.874	89.36
60° C	Blank	477.5	188.0	120.2	30.63	--
	POM	493	251.2	67.97	5.440	82.24

The Arrhenius plots were represented in Fig. 9. The activation parameters were calculated from Arrhenius equation [55].

$$W_{corr} = A e^{-\frac{E_a}{RT}} \quad (5)$$

where E_a is the activation energy and I_{corr} is the corrosion rate for the corrosion of SS in 1.0M H₂SO₄, R is gas constant equal to 8.314 J · K⁻¹ · mol⁻¹, A is the Arrhenius factor, T is absolute temperature.

A rise in the activation energy is explained due to physical adsorption, while unchanged or lowered energy is explained as being indicative to the existence of chemisorption [56].

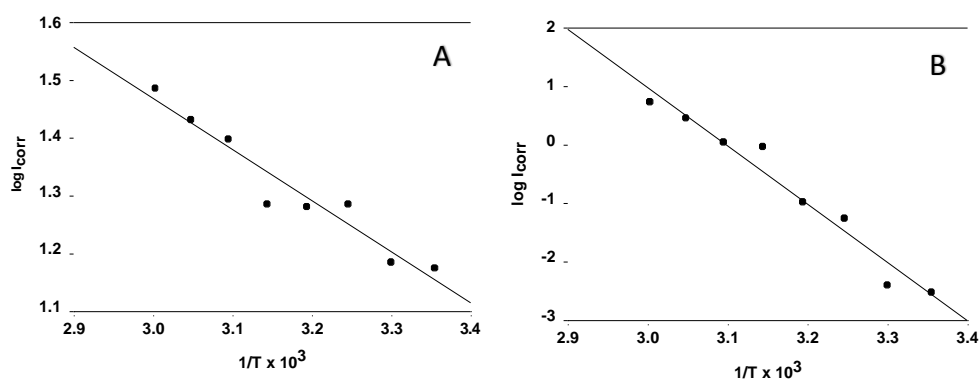


Fig. 9: Arrhenius relationship of the corrosion rates ($\log I_{corr}$) against $1/T$ for SS sample in 1.0 M H₂SO₄ at various temperatures, (A) blank and (B) coated with POM-ILs, from PDP measurements.

The decrease of the $IE\%$ with temperature rise. It expressed by a higher value of $E_a = 190.71$ kJ/mol with POM-ILs, when compared to that in an acid with no coating $E_a = 16.93$ kJ/mol [57-60], (Table 7), is interpreted as indicating a potent action of the inhibition for the studied POM-ILs by growing the energy barrier for the process of SS corrosion [61]. The increase of E_a in the coated SS indicated the weak chemical bonding between POM-ILs molecules and SS surface or physical adsorption [53,62-64] or due to decrease of POM-ILs molecules adsorbed on the SS surface with rising temperature [65]. *Enthalpy* (ΔH) and *entropy* (ΔS) were calculated from Arrhenius transition theory [63] and recorded in Table 7:

$$\log I_{corr}/T = \log (R/Nh) + \Delta S / 2.303 R - \Delta H / 2.303 RT \quad (6)$$

$h = 6.62607004 \times 10^{-34}$ m² kg / s is Planck's constant, $N=6.022 \times 10^{23}$ atom is Avogadro's number =.

Figure 10 showed the plot of $\log I_{corr}/T$ vs. $10^3/T$. The obtained lines with a slope equal to $-\Delta H / 2.303 R$ and an intercept equal to $[\log (R/Nh) + \Delta S / 2.303 R]$ from which the values of ΔS and ΔH have been calculated. The positive signal of the enthalpies (ΔH) in the presence and absence of POM-ILs reflect the endothermic dissolution process of the SS sample and it points that the SS dissolution is difficult [66,67]. The presence of POM-ILs coating reveals that the corrosion process becomes less value of ΔH when compared to blank (Tables 7) indicates that the coating of SS leads to decrease in the enthalpy ΔH than that of uncoated metal, suggestive of a big protection efficiency observed for the SS coating system with POM-ILs [57].

The entropy values (ΔS) is positive, indicating that the reaction was dissociation instead of association [62]. ΔS in the presence of POM-ILs have less value than that in the solution without coating, which implies that disturbance on SS surface decreased in the presence of coating [63].

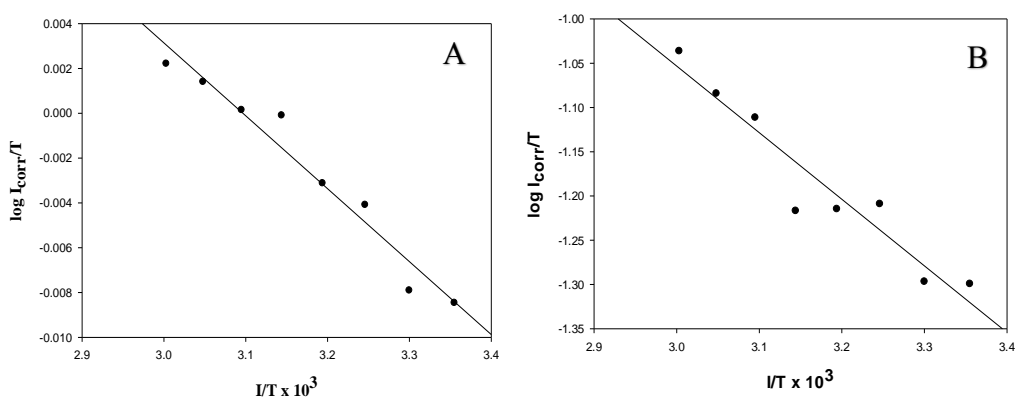


Figure 10: Transition-state plots for SS corrosion rates ($\log I_{corr}/T$) against $1/T$ for SS sample 1.0 M H_2SO_4 at various temperatures, (A) blank and (B) coated with POM-ILs, from PDP measurements

Table 7: Thermodynamic parameters for SS in the presence and absence of POM-ILs in 1.0 M H_2SO_4 at different temperatures

Sample	E_a (kJ.mol ⁻¹)	ΔH (kJ.mol ⁻¹)	ΔS (kJ.mol ⁻¹)
Blank	16.93	14.40	20.37
Coating POM-ILs	190.71	0.624	0.752

Conclusion

In this work we have prepared and characterized Keggin polyoxometalate ionic liquid (POM-IL) ($n-C_7H_{15}_4N)_5[PW_{11}O_{39}Cu(H_2O)]$ and used it as anticorrosion coating for the protection of *stainless steel* metal surface. The synthesized POM-IL based material meet the required characteristics of an efficient coating which are hydrophobicity, stability, effective cost, ease of synthesis, non-toxicity, etc. They also have shown interesting mechanical and chemical corrosion protection of SS surface against sulfuric acid. SEM/EDS surface analysis confirms the stability of POM- based coating, as well as, its efficiency in preventing corrosion.

EIS and PDP electrochemical measurements showed that the presence of the POM-IL coating inhibits SS metal corrosion in acidic media with a protection efficiency of ~ 99 %. The inhibition efficiency is generally stable in different concentrations of H₂SO₄ [0.25 – 1.0 M] and different immersion times [1.0-24.0h] but it decreases when increasing the time of immersion.

Thermodynamic parameters calculated from PDP measurements indicated that activation energy barrier of the corrosion process increases in the presence of POM-IL coating. The results showed that corrosion resistance is stable with different temperature from 25° to 40° C, at higher temperatures, a decrease in the inhibition efficiency is noticed (82.2% at 60 °C) and may be attributed to a partial desorption of the coating from the metallic surface.

References

1. G. Mengoli, M.M. Musiani, B. Pelli, E. Vecchi, Anodic synthesis of sulfur-bridged polyaniline coatings onto Fe sheets. *Journal of Applied Polymer Science* 28 (3) (1983) 1125. doi:10.1002/app.1983.070280318
2. A. Ostovari, SM. Hoseinieh, M. Peikari, SR. Shadzadeh, SJ. Hashemi, Corrosion inhibition of mild steel in 1M HCl solution by henna extract: A comparative study of the inhibition by henna and its constituents (Lawsonic acid, Gallic acid, α -D-Glucose and Tannic acid). *Corrosion Science* 51 (9) (2009) 1935-1949. doi:<https://doi.org/10.1016/j.corsci.2009.05.024>
3. SC. Nwanonenyi, HC. *Chemistry Africa*. doi:10.1007/s42250-018-00035-w
4. F. Kandemirli, S. Sagdinc, Theoretical study of corrosion inhibition of amides and thiosemicarbazones. *Corrosion Science* 49 (5) (2007) 2118-2130. doi:doi.org/10.1016/j.corsci.2006.10.026
5. H. J. Leidheiser, Coatings, Corrosion Mechanisms .In: (ed.) FM (ed) Corrosion Mechanisms. *Marcel Dekker, New York* , (1987)
6. J. Bruzaud, J. Tarrade, E. Celia, T. Darmanin, E. Taffin de Givenchy, F. Guittard, J-M. Herry, M. Guilbaud, M-N. Bellon- Fontaine, The design of superhydrophobic stainless steel surfaces by controlling nanostructures: A key parameter to reduce the implantation of pathogenic bacteria. *Materials Science and Engineering: C* 73 (2017) 40-47. <https://doi.org/10.1016/j.msec.2016.11.115>
7. C-L. Chen, Sutrisna, Study of W-Co ODS coating on stainless steels by mechanical alloying. *Surface and Coatings Technology* 350 (2018) 954-961. <https://doi.org/10.1016/j.surfcoat.2018.03.047>
8. ML. Zheludkevich, IM. Salvado, MGS. Ferreira, Sol-gel coatings for corrosion protection of metals. *Journal of Materials Chemistry* 15 (48) (2005) 5099-5111. doi:10.1039/B419153F
9. A. Mitra, Z. Wang, T. Cao, H. Wang, L. Huang, Y. Yan, Synthesis and Corrosion Resistance of High-Silica Zeolite MTW, BEA, and MFI Coatings on Steel and Aluminum. *Journal of The Electrochemical Society* 149 (10) (2002) B472-B478. doi:10.1149/1.1507784
10. DR. MacFarlane, M. Forsyth, PC. Howlett, JM. Pringle, J. Sun, G. Annat, W. Neil, EI. Izgorodina, Ionic Liquids in Electrochemical Devices and Processes: Managing Interfacial Electrochemistry. *Accounts of Chemical Research* 40 (11) (2007) 1165-1173. doi:10.1021/ar7000952
11. S. Herrmann, A. Seliverstov, C. Streb, Polyoxometalate-ionic liquids (pom-ils)—the ultimate soft polyoxometalates? A critical perspective. *Journal of Molecular and Engineering Materials* 02 .1440001 (01) (2014) doi:10.1142/s2251237314400012
12. DE. Katsoulis, A Survey of Applications of Polyoxometalates. *Chemical Reviews* 98 (1) (1998) 359-388. doi:10.1021/cr960398a
13. S. Lomakina, T. Shatova, L. Kazansky Heteropoly anions as corrosion inhibitors for aluminium in high temperature water. *Corrosion science* 36 (9) (1994) 1645-1651
14. AY. Pikel'nyl, GG. Reznikova, AP. Brynza, SA. Khmelovskaya, OA. Pikel'naya, Electrochemical behavior and corrosion of steel in the presence of some heteropolycompounds. *Russian journal of electrochemistry* 31 (5) (1995) 484-486
15. AY. Pikel'nyi, GG. Reznikova, AP. Brynza, SA. Khmelovskaya, The kinetics and mechanism of corrosion in the presence of heteropolycompounds. *Protection of Metals* (1994) 358-386
16. C. Besecker, W. Marritt, Patent 4900853 A, 1990. 134256. 113. In: *Chem. Abstr*, 1990. p 134256
17. Y. Shindo, M. Kabeya, K. Tanimura, F. Yamazaki Japanese Patent JP 05311457 A2, 1993. 223581n. 120. In: *Chem. Abstr*, 1993. p 223581n
18. W. Jenkins, C. Keemer, H. Lamborn, M. Curcio Patent 535 .122 . 1994.268214 ,6469 In: *Chem. Abstr*, 1994. p 268214
19. H. Ke Ping, F. Jing Li, A protective coating of P-Mo-V heteropoly acid on steel. *Journal of Electron Spectroscopy and Related Phenomena* 83 (1) (1997) 93-98. [https://doi.org/10.1016/S0368-20481-03055\(96\)](https://doi.org/10.1016/S0368-20481-03055(96))
20. I. Perissi, et al., High temperature corrosion properties of ionic liquids. *Corrosion Science*, 48(9) (2006) 2349-2362.

21. N. Birbilis, et al., Exploring corrosion protection of Mg via ionic liquid pretreatment. *Surface and Coatings Technology*, 201(8) (2007) 4496-4504.
22. S. Caporali, et al., Aluminium electroplated from ionic liquids as protective coating against steel corrosion. *Corrosion Science*, 50(2) (2008) 534-539.
23. L.X. Zhang Lancui, Cui Lixin., Evaluation of the corrosion inhibition of ammonium polyoxometalates with Keggin structures. *INDUSTRIAL WATER TREATMENT*, 29(12) (2009) 52-55.
24. Q. Zhang, and Y. Hua, Corrosion inhibition of mild steel by alkylimidazolium ionic liquids in hydrochloric acid. *Electrochimica Acta*, 54(6) (2009) 1881-1887.
25. Q. Zhang, and Y. Hua, Corrosion inhibition of aluminum in hydrochloric acid solution by alkylimidazolium ionic liquids. *Materials Chemistry and Physics*, 119(1) (2010) 57-64.
26. X. Zhou, H. Yang, and F. Wang, [BMIM]BF₄ ionic liquids as effective inhibitor for carbon steel in alkaline chloride solution. *Electrochimica Acta*, 56(11) (2011) 4268-4275.
27. P. Arellanes-Lozada, et al., Evaluation of the corrosion inhibiting effect of an ionic liquid (N-dimethyl- N-di (cocoalkyl) ammonium methyl sulfate) on API 5L X52 steel in hydrochloric acid, *Int J Electrochem Sci*, 10 (2015) 2776-2790.
28. A.M. El-Shamy, et al., Anti-bacterial and anti-corrosion effects of the ionic liquid 1-butyl-1-methylpyrrolidinium trifluoromethylsulfonate. *Journal of Molecular Liquids*, 211 (2015) 363-369.
29. A.P. Hanza, et al., Corrosion behavior of mild steel in H₂SO₄ solution with 1, 4-di [1'-methylene-3'- methyl imidazolium bromide]-benzene as an ionic liquid. *Corrosion Science*, 107 (2016) 96-106.
30. Y. Qiang, et al., Experimental and theoretical studies of four allyl imidazolium-based ionic liquids as green inhibitors for copper corrosion in sulfuric acid. *Corrosion Science*, 119 (2017) 68-78.
31. S. Kshama Shetty and A. Nityananda Shetty, Eco-friendly benzimidazolium based ionic liquid as a corrosion inhibitor for aluminum alloy composite in acidic media. *Journal of Molecular Liquids*, 225 (2017) 426- 438.
32. F. El-Hajjaji et al., Pyridazinium-based ionic liquids as novel and green corrosion inhibitors of carbon steel in acid medium: Electrochemical and molecular dynamics simulation studies. *Journal of Molecular Liquids*, 249 (2018) 997-1008.
33. S. Herrmann, M. Kostrzewa, A. Wierschem, Streb C Polyoxometalate Ionic Liquids as Self-Repairing Acid-Resistant Corrosion Protection. *Angewandte Chemie International Edition* 53 (49) (2014) 13596-13599. doi:10.1002/anie.201408171
34. KT. Venkateswara Rao, B. Haribabu, PS. Sai Prasad, N. Lingaiah, Vapor-phase selective aerobic oxidation of benzylamine to dibenzylimine over silica-supported vanadium-substituted tungstophosphoric acid catalyst. *Green Chemistry* 15 (3) (2013) 837-846. doi:10.1039/C3GC36735E
35. F. El-Taib Heakal, S. Haruyama *Corros. Sci.*, 20 (1980) 887-898.
36. K. Aramaki, Semi-Quantitative Evaluation of Steric Effect on Corrosion Inhibition Efficiency of Branched Alkyl Amines. *CORROSION ENGINEERING* 26 (6) (1977) 297-303
37. Z. Szklarska-Smialowska, G. Wieczorek , Adsorption isotherms on mild steel in H₂SO₄ solutions for primary aliphatic compounds differing in length of the chain. *Corrosion Science* 11 (11) (1971) 843-852. doi:[https://doi.org/10.1016/S0010-938X\(71\)80048-3](https://doi.org/10.1016/S0010-938X(71)80048-3)
38. M. W. Kendig, A. T. Allen, S. Jeanjaquet and F. Mansfeld, In *Electrochemical Techniques for Corrosion Engineering*, Ed. R. Badoian, NACE (1986).
39. J. R. McDonald, Impedance Spectroscopy, *John Wiley & Sons, New York*. 37 (1987).
40. T. Tsurus, S. Haruyama, Corrosion monitor based on impedance method. II. Construction and its application to homogeneous corrosion. *Journal of Japan Society of Corrosion Engineering* 27 (1978) 573-579
41. H. Ma, X. Cheng, S. Chen, C. Wang, J. Zhang. and H. Yang, An ac impedance study of the anodic dissolution of iron in sulfuric acid solution containing hydrogen sulfide, *J. Electroanal. Chem.*, 451 (1998) 11.
42. D.T. Chin and H. H. Chang, On the conductivity of phosphoric acid electrolyte', *J. Appl. Electrochem.*, 19 (1989) 95-99.
43. G. Lewis, P. G. Fox and P. J. Boden, The corrosion of Fe-12Cr iron-chromium alloys in H₃PO₄, *Corros. Sci.*, 20 (1980) 331-339.
44. A. Fouda and M. El-Semongym, *J. Indian Chem. Soc.*, 59, (1982) 9.
45. E. Hopson, K. Tales, Iron Fever, The Iron Industry Permeates Kent. Kent, Ct: The Kent Historical Society (1990)
46. E.E. Ebenso, Effect of halide ions on the corrosion inhibition of mild steel in H₂ SO₄ using methyl red - Part 1 *Bull. Electrochem.*, 19 (2003) 209.
47. M.S. Morad, A.M.K. El-Dean, 2,2'-Dithiobis(3-cyano-4,6-dimethylpyridine): A new class of acid corrosion inhibitors for mild steel, *Corros. Sci.*, 48 (2006) 3398-3412. <https://doi.org/10.1016/j.corosci.2005.12.006>
48. V. Likhanova, A. Marco Dominguez-Aguilar, Octavio Olivares-Xometl, Noel Nava-Entazana, Elsa Arce,

- Hector Dorantes, The effect of ionic liquids with imidazolium and pyridinium cations on the corrosion inhibition of mild steel in acidic environment, *Corros. Sci.* 52 (2010) 2088-2097. <https://doi.org/10.1016/j.corsci.2010.02.030>
49. H.H. Uhlig RWRa, corrosion and corrosion control. 4 edn. *John Wiley & Sons*, (2008).
 50. M. Abdallah, Corrosion kinetics of carbon steel in HCl solutions and the effect of some ethoxylated fatty amines as corrosion inhibitors. *Annali di chimica* 84539-529 (1994) (12-11)
 51. S. Rengamani, T. Vasudevan, S. Venkatakrishna Iyer, Beta phenylethylamine as an inhibitor for corrosion of mild steel in acidic solutions. *Indian Journal of Technology* 31 (7) (1993) 519-524
 52. R. Solmaz, Investigation of the inhibition effect of 5-((E)-4-phenylbuta-1, 3-dienylideneamino)-1, 3, 4-thiadiazole-2-thiol Schiff base on mild steel corrosion in hydrochloric acid, *Corrosion Science* 52 (10) (2010) 3321- 3330
 53. S. Muralidharan, BR. Babu, SV. S. Iyer, Rengamani, Influence of anions on the performance of isomers of aminobenzoic acid on the corrosion inhibition and hydrogen permeation through mild steel in acidic solutions. *Journal of Applied Electrochemistry* 26 (3) (1996) 291-296
 54. Ü. Ergun, D. Yüzer, KC. Emregül, The inhibitory effect of bis-2,6-(3,5-dimethylpyrazolyl)pyridine on the corrosion behaviour of mild steel in HCl solution. *Materials Chemistry and Physics* 109 (2) (2008) 492-499. <https://doi.org/10.1016/j.matchemphys.2007.12.023>
 55. I.N. Putilova, S.A. Balezin, V.P. Barannik, *Metallic Corrosion Inhibitors*, Pergamon Press, New York (1960) p. 31.
 56. T. Szauer, A. Brandt, On the role of fatty acid in adsorption and corrosion inhibition of iron by amine— fatty acid salts in acidic solution. *Electrochimica Acta* 26 (9) (1981) 1257-1260. doi:[https://doi.org/10.1016/0013-4686\(80-85108\)1](https://doi.org/10.1016/0013-4686(80-85108)1)
 57. E. Khamis, A. Hefnawy, A. M. El-Demerdash, Acid Cleaning of Steel Using Arghel Echo Friendly Corrosion Inhibitor. *Material wissenschaft und Werkstoff technik* 38 (3) (2007) 227-232. doi:10.1002/mawe.200600097
 58. O. U. Abakedi, V. F. Ekpo, E.E. John, Corrosion inhibition of mild steel by Stachytarpheta indica leaf extract in acid medium. *The Pharmaceutical and Chemical Journal* 3 (1) (2016) 165-171.
 59. I.Y. Suleiman, M. Abdulwahab, F.E. Awe, “A study of The Green Corrosion Inhibition of Acacia tortilis Extract on Mild Steel Sulphuric Acid Environment”, *J. Advanced Electrochem.*, 2(1) (2016) 50-55.
 60. L. El Hattabi, S. Echihi, M. El Fal, A. Guenbour, Y. Ramli, E. Essassi, M. Tabyaoui, Electrochemical and quantum chemical study of 1-ethyl-1H-pyrazolo [3, 4-d] pyrimidine-4 (5H)-thione as corrosion inhibitor for mild steel in HCl solution. *Journal of Materials and Environmental Sciences* 8 (7) (2017) 2428-2441.
 61. E. A. Noor, A. H. Al-Moubaraki, Thermodynamic study of metal corrosion and inhibitor adsorption processes in mild steel/1-methyl-4[4'(-X)-styryl pyridinium iodides/hydrochloric acid systems. *Materials Chemistry and Physics* 110 (1) (2008) 145-154. doi:<https://doi.org/10.1016/j.matchemphys.2008.01.028>
 62. L. Larabi, Y. Harek, O. Benali, S. Ghalem, Hydrazide derivatives as corrosion inhibitors for mild steel in 1 M HCl, *Prog Org Coa.*, t 54 (2005) 256-262
 63. L. Larabi, O. Benali, Y. Harek, Corrosion inhibition of cold rolled steel in 1 M HClO₄ solutions by N- naphthyl NO -phenylthiourea, *Mat Lett.*, 61 (2007) 3287–3291
 64. E. A. Noor, A. H. Al-Moubaraki, Thermodynamic study of metal corrosion and inhibitor adsorption processes in mild steel/1-methyl-4[4'(-X)-styryl pyridinium iodides/hydrochloric acid systems *Mater. Chem. Phys.*, 110(2008) 145-154.
 65. T. Szauer, A. Brandt, Adsorption of Oleates of various amines on iron in acidic solution, *Electrochim. Acta*, 26 (1981) 1209-1217.
 66. A. Zarrouk, M. Messali, H. Zarrok, R. Salghi, A. Ali, B. Hammouti, S. Al-Deyab, F. Bentiss, Synthesis, characterization and comparative study of new functionalized imidazolium-based ionic liquids derivatives towards corrosion of C38 steel in molar hydrochloric acid. *Int. J. Electrochem. Sci.* 7 (2012) 6998
 67. N.M. Guan, L. Xueminh, L. Fei. *Mater. Chem. Phys.* 58(11) (2004) 1768-1772.
 68. A. M. Abdel-Gaber, E. Khamis, H. Abo-ElDahab, S .Adeel, Inhiition of aluminum corrosion in alkaline solutions using natural compound”, *Mater. Chem. Phys.*, 109 (2008) 297-305.
 69. M. Yadav, S. Kumar, R. R. Sinha, D. Beehra, Experimental and quantum chemical studies on corrosion inhibition performance of Benzimidazole derivatives for mild steel in HCl, *Ind. Eng. Chem. Res.*, 52 (2013) 6318-6328.

(2019) ; <http://www.jmaterenvirosci.com>